JACS
JOURNAL OF THE AMERICAN CHEMICAL SOCIETY

ARTICLE

pubs.acs.org/JACS

Organic Redox Couples and Organic Counter Electrode for Efficient Organic Dye-Sensitized Solar Cells

Haining Tian,[†] Ze Yu,[‡] Anders Hagfeldt,[§,⊥] Lars Kloo,[*,‡,⊥] and Licheng Sun[*,†,⊥]

[†]Organic Chemistry, Center of Molecular Devices, Department of Chemistry, School of Chemical Science and Engineering, Royal Institute of Technology (KTH), SE-10044 Stockholm, Sweden

[‡]Inorganic Chemistry, Center of Molecular Devices, Department of Chemistry, School of Chemical Science and Engineering, Royal Institute of Technology (KTH), SE-10044 Stockholm, Sweden

[§]Department of Physical and Analytical Chemistry, Uppsala University, SE-75105 Uppsala, Sweden

[⊥]State Key Laboratory of Fine Chemicals, DUT-KTH Joint Education and Research Center for Molecular Devices, Dalian University of Technology (DUT), 116012 Dalian, China

Supporting Information

ABSTRACT: A series of organic thiolate/disulfide redox couples have been synthesized and have been studied systematically in dye-sensitized solar cells (DSCs) on the basis of an organic dye (TH305). Photophysical, photoelectrochemical, and photovoltaic measurements were performed in order to get insights into the effects of different redox couples on the performance of DSCs. The polymeric, organic poly(3,4-ethylenedioxythiophene) (PEDOT) material has also been introduced as counter electrode in this kind of noniodine-containing DSCs showing a promising conversion efficiency of 6.0% under AM 1.5G, 100 mW·cm^{-2} light illumination. Detailed studies using electrochemical impedance spectroscopy and linear-sweep voltammetry reveal that the reduction of disulfide species is more efficient on the PEDOT counter electrode surface than on the commonly used platinized conducting glass electrode. Both pure and solvated ionic-liquid electrolytes based on a thiolate anion have been studied in the DSCs. The pure and solvated ionic-liquid-based electrolytes containing an organic redox couple render efficiencies of 3.4% and 1.2% under 10 mW·cm^{-2} light illumination, respectively.

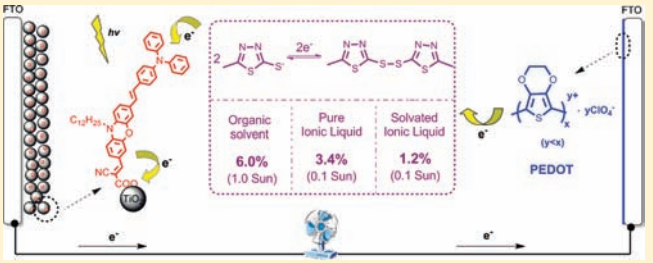

INTRODUCTION

Dye-sensitized solar cells (DSCs), significantly improved by O'Regan and Grätzel in 1991, represent a simple, efficient, and economical photovoltaic device based on a new strategy for solar energy-to-electricity conversion.[1] Like other electrochemical devices, the DSCs consist of three main components: a photoactive working electrode (WE), a counter electrode (CE), and a redox-active electrolyte to connect the electrodes. In recent years, many attempts have been made to optimize this device from essentially every possible aspect.[2] The replacement of the ubiquitous I^-/I_3^- electrolyte redox couple would be a critical improvement because of its disadvantages in terms of corrosion of metal-based current collectors (especially for silver), evaporation losses, and visible light absorption.[3] Until now, three main kinds of iodine-free liquid electrolytes, based on metal complexes,[4−13] inorganic materials,[14−22] or organic redox couples,[3,7,23−32] have been developed for the DSCs. One of the organic redox couples, the thiolate/disulfide system with multielectron-transfer capability, has shown potential applications in lithium-ion batteries as well as in DSC electrolytes.[3,25,26,33,34] Recently, Wang et al. reported an interesting thiolate/disulfide redox couple derived from 5-mercapto-1-methyltetrazole, which showed an efficiency of 6.4% together with a ruthenium-based dye (Z907Na) in DSCs under standard illumination conditions (100 mW·cm^{-2}).[3] For DSCs fabricated with an organic dye (TH305[35]), our group has adopted a sulfide-based redox couple derived from mercapto-5-methyl-1,3,4-thiadiazole (McMT), which showed a 4.0% efficiency.[26] On the other hand, Li et al. applied tetramethylthiourea derivatives to N3 dye-based DSCs and obtained 3.1% efficiency using a carbon counter electrode.[25] Liu et al. used the same organic redox couple in organic D131 dye-based DSCs, which shows 3.9% efficiency on the basis of a carbon CE under standard light illumination.[32] Just as for the photosensitizers, structural modification may finetune the physical and electrochemical properties of the thiolate/disulfide redox couples, which significantly can affect the photovoltaic properties of DSCs. Also, according to a previous study, the fill factor (*ff*) of the DSCs based on this thiolate/disulfide electrolyte is very low because of a large reduction resistance of the disulfide on the standard platinized CE leading to a decrease in the overall conversion efficiency of the DSCs.[26] This implies that platinum is not a suitable catalytic material for thiolate/disulfide electrolyte reduction at the CE. Thus, a more effective counter electrode material is required. Although some efforts have been

Received: February 9, 2011
Published: May 18, 2011

dx.doi.org/10.1021/ja2030933 | J. Am. Chem. Soc. 2011, 133, 9413–9422

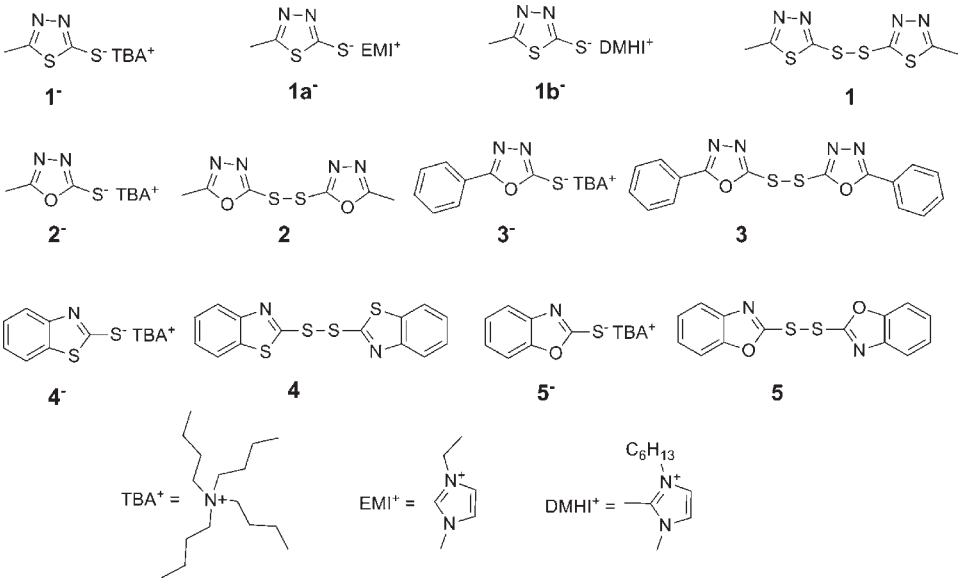

Figure 1. Structures of the compounds used in the organic redox couples.

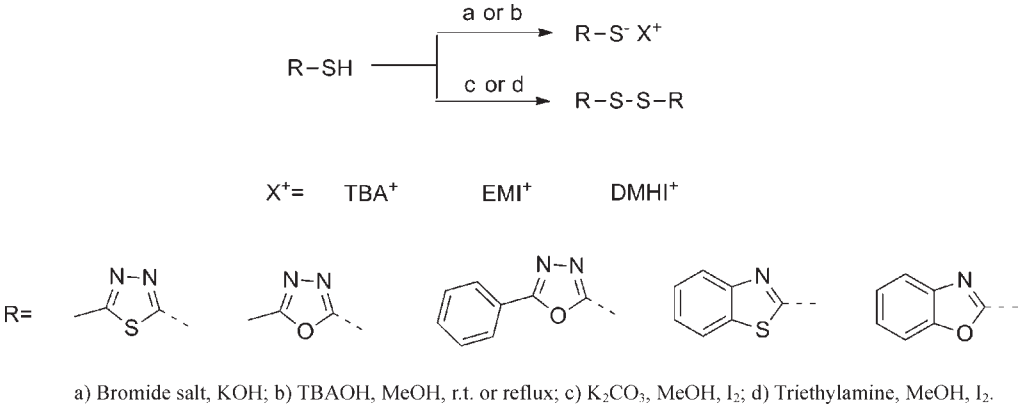

Figure 2. The general synthetic routes of the compounds used in the organic redox couples.

made to use a carbon-based electrode for the thiolate/disulfide redox couple, the *ff* is still not satisfactory.[25,32] In this paper, we report the successful development of a series of thiolate/disulfide redox couples (see Figure 1) and further a systematic study of the effect of redox couple structures on the photovoltaic properties of DSCs on the basis of the TH305 organic dye. Furthermore, owing to the poineering work on the poly(3,4-ethylenedioxythiophene) (PEDOT) material for lithium-ion batteries and DSCs,[30,33,34,36−46] we have also adopted the PEDOT material as CEs prepared by electrochemical polymerization in organic dye-sensitized solar cells on the basis of thiolate/disulfide electrolytes. Subsequently, we have investigated the essential differences between platinized conducting glass and PEDOT as substrates for disulfide reduction. Meanwhile, pure imidazolium ionic-liquid electrolytes and solvated ionic liquid based on thiolate anions have been prepared and applied to DSCs and have been characterized by photophysical and photovoltaic techniques.

RESULTS AND DISCUSSIONS

1. Synthesis. The synthetic routes of the organic redox couples are depicted in Figure 2. All of the thiolate species were obtained by neutralization of the corresponding mercaptan using hydroxide compound, and the disulfide compounds were obtained through oxidation of the corresponding mercaptan by iodine in basic solution. Thiolates $\mathbf{1a}^-$ and $\mathbf{1b}^-$ are ionic liquids at room temperature. The synthesis details of these redox couples are presented in the Supporting Information. The disulfide **2** is very sensitive to oxygen and can easily be further oxidized to the corresponding sulfoxid. Therefore, the fresh disulfide **2** has to be used in all measurements.

2. Different Redox Couples. The redox potential is one of the most important parameters of redox couples in DSCs. To determine the standard redox potentials of the organic redox couples, cyclic voltammetric (CV) measurements were performed using 0.2 M $LiClO_4$ as supporting electrolyte at 20 °C at a scan rate of 50 $mV \cdot s^{-1}$. For the $\mathbf{1}^-/\mathbf{1}$, $\mathbf{2}^-/\mathbf{2}$, and $\mathbf{5}^-/\mathbf{5}$ redox couples, the solution studied contained 20 mM of the reduced component and 10 mM of the oxidized component in acetonitrile (MeCN). Because of the poor solubility of **3** and **4** in MeCN, for the $\mathbf{3}^-/\mathbf{3}$ redox couple, the solution contained 20 mM of $\mathbf{3}^-$ and was saturated with respect to **3** in MeCN. However, for the $\mathbf{4}^-/\mathbf{4}$ redox couple, the solution consisted of 20 mM of $\mathbf{4}^-$ and was saturated with **4** in DMSO/DMF (6/4; v/v). The potential

dx.doi.org/10.1021/ja2030933 |*J. Am. Chem. Soc.* 2011, 133, 9413–9422

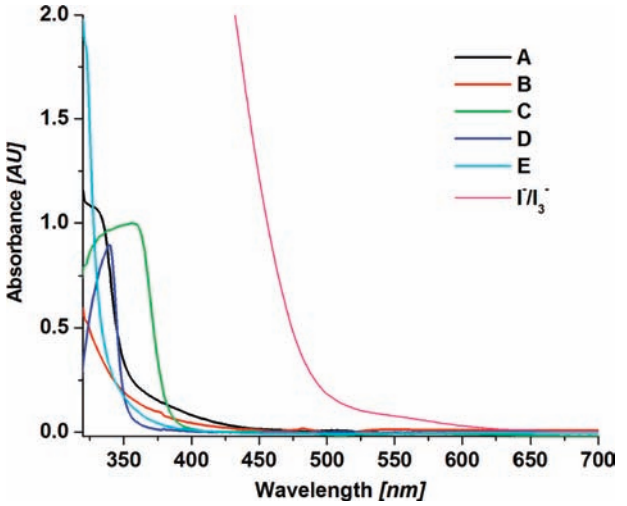

Figure 3. UV−vis spectra of a thin layer of different electrolytes confined between two conducting glass substrates sealed with 25 μm Surlyn film.

versus the normal hydrogen electrode (NHE) was calibrated using the reference Ferrocene/Ferrocenium (Fc/Fc^+) redox couple by introducing a correction of 630 mV.[48] From the CV curves of these redox couples (Figure S1 of the Supporting Information), the redox potentials of $\mathbf{1}^-/\mathbf{1}$, $\mathbf{2}^-/\mathbf{2}$, $\mathbf{3}^-/\mathbf{3}$, $\mathbf{4}^-/\mathbf{4}$, and $\mathbf{5}^-/\mathbf{5}$ were determined to 0.15, 0.25, 0.37, 0.01, and 0.29 V versus NHE, respectively. For the compounds with a similar structure ($\mathbf{1}^-/\mathbf{1}$ and $\mathbf{2}^-/\mathbf{2}$, $\mathbf{4}^-/\mathbf{4}$ and $\mathbf{5}^-/\mathbf{5}$, respectively), changing a S atom to O in the molecular framework makes the redox potential more positive and, thus, the system more oxidizing. Compared with $\mathbf{2}^-/\mathbf{2}$, $\mathbf{4}^-/\mathbf{4}$ containing extra phenyl groups also gives a more positive redox potential probably because of the stronger electron-withdrawing ability of the phenyl group as compared to the methyl group in the $\mathbf{2}^-/\mathbf{2}$ redox couple.

The electrolytes **A**, **B**, **C**, **D**, and **E** were prepared from the $\mathbf{1}^-/\mathbf{1}$, $\mathbf{2}^-/\mathbf{2}$, $\mathbf{3}^-/\mathbf{3}$, $\mathbf{4}^-/\mathbf{4}$, and $\mathbf{5}^-/\mathbf{5}$ redox couples in a mixed MeCN/ethylene carbonate (EC) (6/4, v/v) solvent, respectively. The electrolytes consisted of 0.2 M of the thiolate species, 0.2 M of the disulfide species ($\mathbf{1}^-/\mathbf{1}$ and $\mathbf{2}^-/\mathbf{2}$), or were saturated with respect to the oxidized species (**3** < 0.02 M, **4** < 0.05 M, and **5** < 0.2 M), 0.05 M $LiClO_4$ and 0.5 M 4-*t*-butylpyridine (TBP). Figure 3 shows the absorption sepctra of a thin layer of the different organic redox couple based electrolytes compared to an electrolyte containing I^-/I_3^- redox couple (0.2 M TBA^+I^-, 0.2 M I_2, 0.05 M $LiClO_4$, and 0.5 M TBP in MeCN/EC (6/4, v/v)) confined between two conducting glass substrates sealed with 25 μm Surlyn film. Thus, the absorption spectra can at least be regarded as semiquantitative. All of the electrolytes containing the organic redox couples essentially display no absorption in the visible part of the spectrum in contrast to the I^-/I_3^- based electrolyte.

For DSC fabrication, the organic dye TH305 was employed as photosensitizer, and optimized platinized fluorine-doped tin oxide (FTO) conducting glass (~8.6 $\mu g \cdot cm^{-2}$) was used as CE. The photocurrent density−photovoltage ($J-V$) curves (Figure 4a) of DSCs based on different organic electrolytes were obtained under 100 $mW \cdot cm^{-2}$ simulated sunlight illumination, and the corresponding photovoltaic properties are collected in Table 1. To further study the effects of different electrolytes on the quasi-Fermi level of TiO_2 ($E_{F,n}$) and electron lifetime in

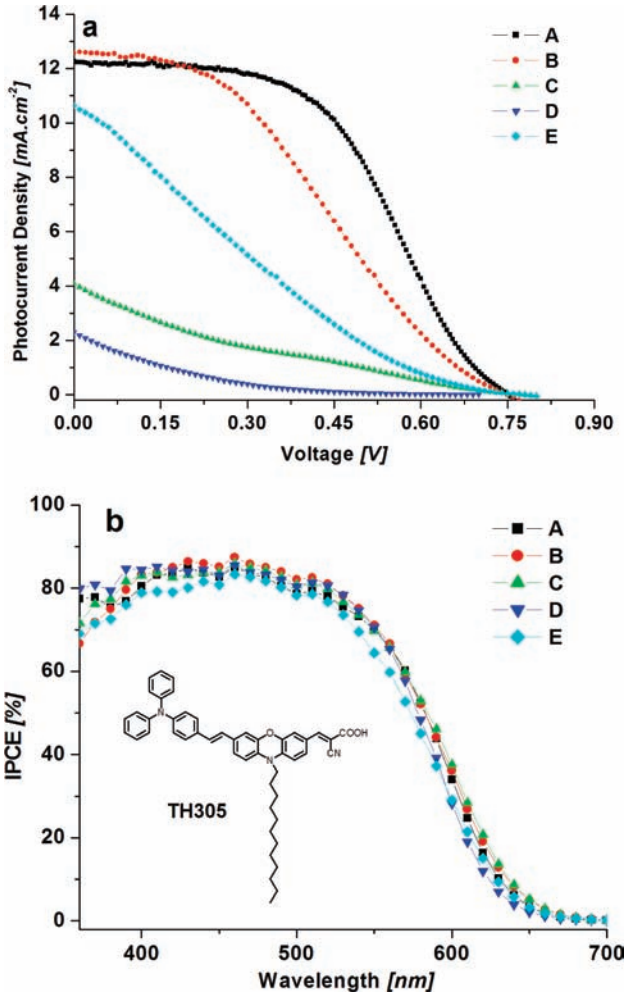

Figure 4. The $J-V$ curves (a) and IPCE spectra (b) of DSCs based on different organic electrolytes.

Table 1. Photovoltaic Properties of TH305-Based DSCs with Different Organic Electrolytes[a]

electrolyte	J_{sc} [$mA \cdot cm^{-2}$]	V_{oc} [mV]	*ff*	η[b] [%]
A	12.3	750	0.50	4.6
B	12.6	750	0.35	3.3
C	4.1	790	0.18	0.6
D	2.3	690	0.10	0.2
E	10.6	780	0.19	1.6

[a] The TiO_2 film consists of 10 μm transparent layer and 2 μm scattering layer. [b] Light intensity is AM 1.5G, 100 $mW \cdot cm^{-2}$.

TiO_2, charge extraction and electron lifetime (see Figure 5) measurements were performed. The quasi-Fermi level ($E_{F,n}$) in TiO_2 was derived from the equation $V_{oc} = |E_{F,n} - E_{redox}|$, where V_{oc} is the open-circuit voltage of the DSC and E_{redox} is the redox potential of the electrolyte. Electrolyte A gives the highest photon-to-electricity conversion efficiency (η) of 4.6% with a short-current density (J_{sc}) of 12.3 $mA \cdot cm^{-2}$, an open-circuit voltage (V_{oc}) of 750 mV, and a fill factor (*ff*) of 0.50. This is in spite of the fact that electrolyte B, with the $\mathbf{2}^-/\mathbf{2}$ redox couple, is characterized by a more positive redox potential, 0.25 V versus NHE, than the $\mathbf{1}^-/\mathbf{1}$ redox couple, 0.15 V versus NHE. The

dx.doi.org/10.1021/ja2030933 |*J. Am. Chem. Soc.* 2011, 133, 9413–9422

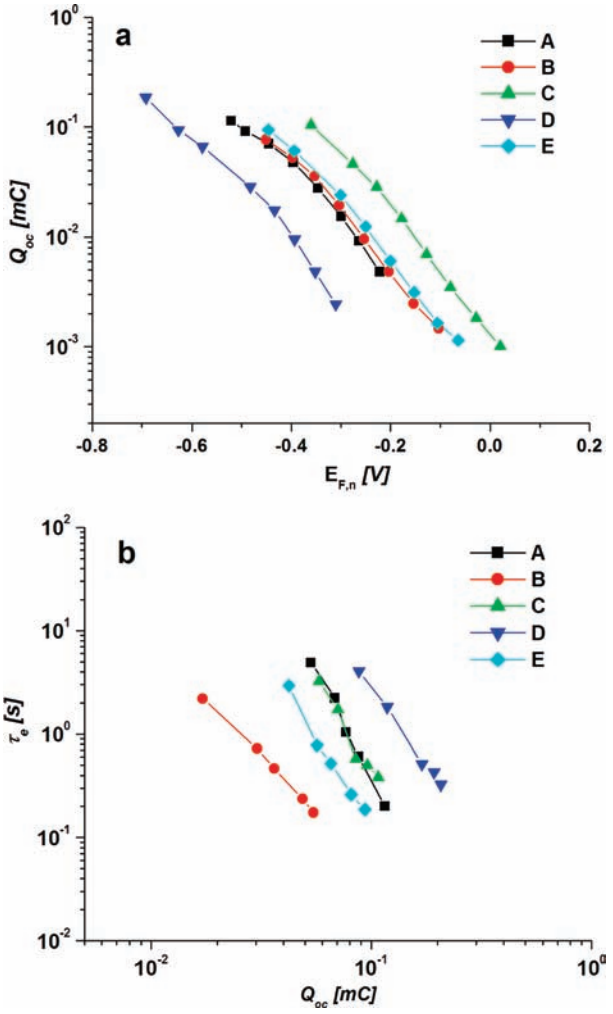

Figure 5. Charge extraction (a) and lifetime (b) of DSCs based on different electrolytes.

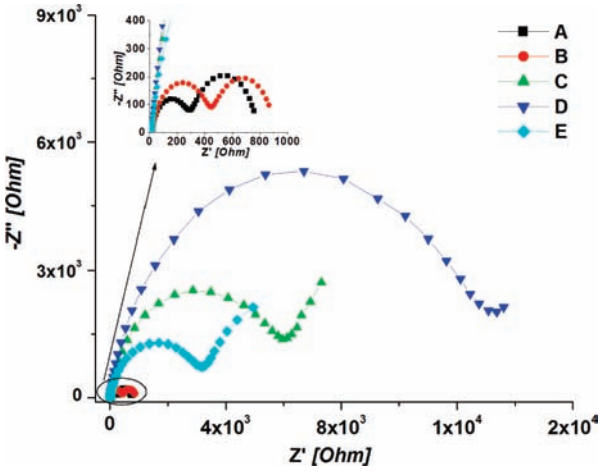

Figure 6. Nyquist plots obtained from DSCs containing the different electrolytes under dark conditions and with an applied bias voltage of −0.7 V.

DSCs based on electrolyte B render about the same photovoltage as those of electrolyte A. According to electron lifetime and charge-extraction results, we can observe that both electrolytes

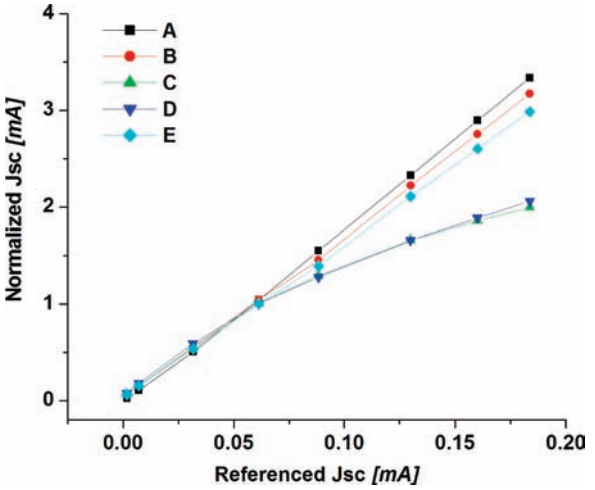

Figure 7. Light-intensity dependence of the current density under short-circuit conditions for DSCs containing the different electrolytes.

show the same effect on the conduction band (CB) of the TiO_2; however, the DSCs containing electrolyte A render a much longer electron lifetime than those containing electrolyte B at a given Q_{oc} value. This indicates that electron recombination losses of injected photoelectrons to electrolyte B are much higher than for electrolyte A. Notably, electrolyte B gives a much lower *ff*, 0.35, than electrolyte A, 0.50. To further investigate the difference between electrolyte A and electrolyte B in DSCs, electrochemical impedance spectroscopy (EIS) measurments were performed under dark conditions and an applied bias voltage of −0.7 V. The Nyquist plots of DSCs based on different electrolytes are shown in Figure 6. From these results, we can observe that DSCs containing the electrolyte A show considerably lower charge-transfer resisitance at the CE (R_{CE}), 320 Ω, as compared to DSCs containing the electrolyte B with an R_{CE} of 500 Ω. This may be the reason for the higher *ff* observed for the electrolyte A. The results indicate that the component **1** more easily reduced on the platinized CEs than the component **2**. Nevertheless, both R_{CE}'s are far too high to give competitive conversion efficiencies, and the main reason can be attributed to the fact that the Pt particles deposited on the FTO glass substrate surface simply do not act as efficient catalysts for the reduction of the disulfide electrolyte species in contrast to iodine/triiodide, the iodine-based electrolyte systems. A general conclusion is that other types of counter electrode materials adapted to the sulfur-based organic redox systems must be identified. The light-intensity dependence of the current density under short-circuit conditions for DSCs with different electrolytes (Figure 7) again identifies the electrolytes A and B as the best working ones showing a linear relationship between DSC photocurrent and light intensity. This implies that there is no serious mass-transport problem in the electrolytes A and B. However, the electrolytes C and D show a clear mass-transport problem that is probably caused by their large molecules as well as by the low concertration of oxidized state species in the electrolytes imposed by their low solubility.

Although no such serious mass-transport problem was found for electrolyte E, the lower *ff* lowered the overall efficiency of such DSCs. The large R_{CE} observed for the electrolytes C−E is the key reason for the low *ff* of DSCs based on these electrolytes. The electrolytes C and D shift the CB position of TiO_2 to more

dx.doi.org/10.1021/ja2030933 |*J. Am. Chem. Soc.* 2011, 133, 9413–9422

positive and negative values, respectively, probably because of different effects on the surface chemistry of titania of these two redox couples. From incident photon-to-current conversion efficiency (IPCE) spectra (Figure 4b), the DSCs based on all of these electrolytes show almost the same active range and values revealing that these electrolytes give similar photocurrents under very low light illumination. On the basis of these results, further modification of this kind of redox couple should focus on solving the mass-transport problem, the solubility of the oxidized component of the redox couple, and the identification of a better counter electrode material to obtain efficient charge transfer.

3. Counter Electrodes. Since the standard type of counter electrode based on platinized FTO, which is optimized for an iodine-based redox electrolyte, obviously is anything but optimized for the sulfur-based redox electrolytes, advanced counter electrode materials have been investigated. The main objective is to introduce a CE material that offers a large effective surface for charge transfer. Obvious candidates involve conducting carbon materials and polymeric materials.[25,30,32] In this section, the performance of PEDOT as counter electrode material is presented and discussed. The PEDOT CEs were prepared by electrochemical polymerization on an FTO conducting glass substrate using the 3,4-ethylenedioxythiophene (EDOT) monomer at a concentration of 20 mM in a 0.1 M $LiClO_4$ solution of MeCN via CV scans amounting to one or two cycles with the sweep rate of 50 $mV \cdot s^{-1}$ over the potential range −0.6 to 1.2 V versus Ag/Ag^+. The UV−vis spectrum of the PEDOT CE (see Figure S2 of the Supporting Information) displays two absorption bands at 400−700 nm and 700−900 nm. According to the literature,[34] the 400−700 nm absorption band is ascribed to the reduced form of PEDOT and the other 700−900 nm band is ascribed to the oxidized form of PEDOT. This means that the PEDOT film prepared under our experimental conditions could be a mixture of the reduced and oxidized forms. The electrolyte used in the investigations of the new CE material is electrolyte A. The DSC devices showed an unexpected efficiency of 6.0% with a J_{sc} value of 12.5 $mA \cdot cm^{-2}$, a V_{oc} value of 745 mV, and an *ff* of 0.65 under 100 $mW \cdot cm^{-2}$ simulated sunlight illumination. This result is comparable to the reported efficiency of 6.4% obtained using ruthenium-dye-based DSCs with another thiolate/disulfide-based electrolyte.[3]

To optimize the PEDOT CEs, one and two CV cycles were introduced to prepare PEDOT CEs. Using a different number of CVs most likely influences both film thickness and morphology. The R_{CE} of DSCs based on PEDOT films prepared by two cycles is much lower than that of DSCs based on PEDOT films prepared by one cycle (see Figure S3 of the Supporting Information) leading to a higher *ff*, 0.65. However, more CV cycles made the PEDOT film too brittle and too weakly attached to the FTO surface. As a result, the films became easy to peel off from the FTO surface, and the interface contact must be rather bad. Consequently, PEDOT films from two CV cycles were used in the following experiments. Noticeably, when a PEDOT film is employed as CE in DSCs, an additional semicircle (2−3 Ω) in the high-frequency region is observed. This effect is likely to originate from the charge-transfer resistance (R_{CE}') at the FTO/PEDOT interface.

The corresponding *J*−*V* curves of DSCs based on platinized FTO and PEDOT CEs are shown in Figure 8. To better understand the reasons for the difference in performance between the PEDOT and platinized FTO CEs in DSCs based on the $\mathbf{1}^-/\mathbf{1}$ redox couple, EIS of DSCs was performed using −0.7 V bias voltage under dark conditions (Figure 9a). Two semicircles are clearly observed in the Nyquist plots of DSCs based on platinized FTO of which the two effects originate from the CE and the dye-sensitized WE, respectively. By fitting the Nyquist plots to an electrochemical model,[49] the electrolyte reduction resistance on CE and the electron recombination resistance from WE of DSCs based on platinized FTO CEs are 320 Ω and 500 Ω, respectively. The WE resistance of DSCs based on PEDOT CEs

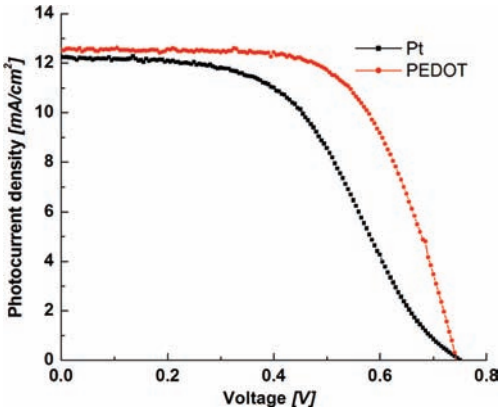

Figure 8. *J*−*V* curves of electrolyte A based DSCs using platinized FTO and PEDOT CEs.

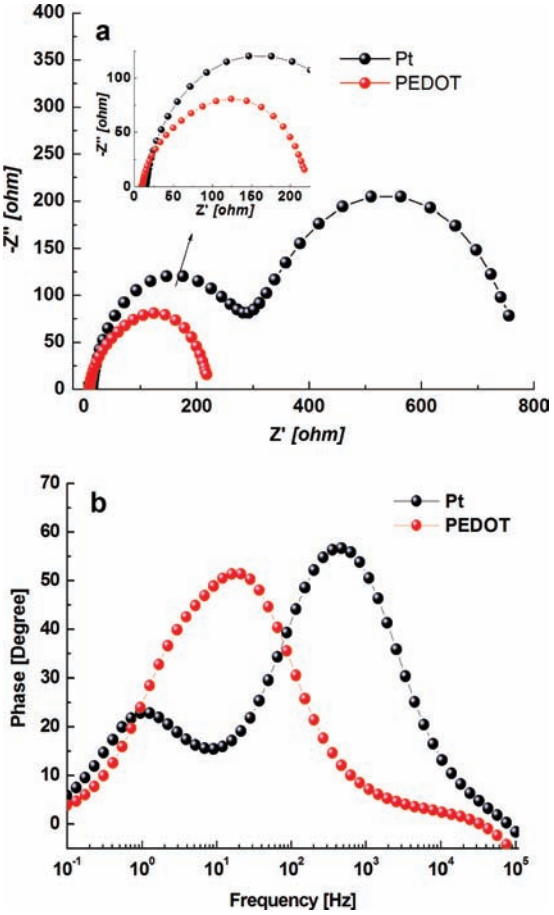

Figure 9. Nyquist (a) and Bode (b) plots of DSCs containing electrolyte A based on platinized FTO and PEDOT CEs with −0.7 V bias voltage.

dx.doi.org/10.1021/ja2030933 |*J. Am. Chem. Soc.* 2011, 133, 9413–9422

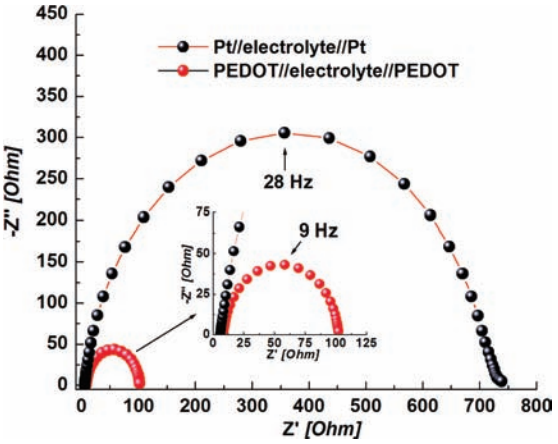

Figure 10. Thin-layer cells based on the CE//electrolyte//CE system with 0 V bias voltage.

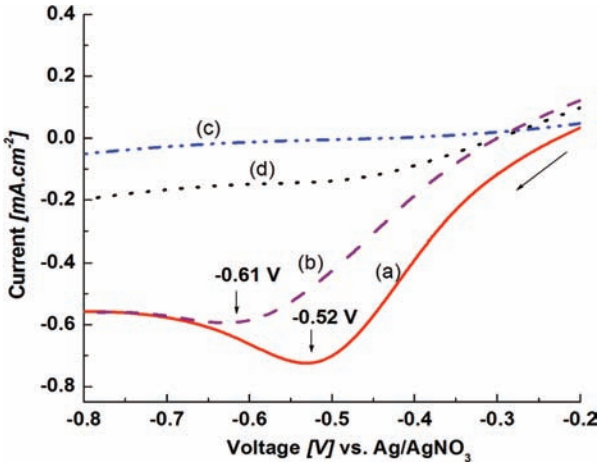

Figure 11. LSV of PEDOT (a), platinized FTO (b), and bare FTO (c) in 2 mM **1**, 0.1 M $LiClO_4$ in MeCN solution, and PEDOT (d) in 0.1 M $LiClO_4$ in MeCN solution.

is ca. 210 Ω. The electron lifetime (τ_e), giving an estimate of the electron recombination rate between the electrolyte and the TiO_2 film, displays a difference between DSCs with a PEDOT CE and a platinized FTO. The τ_e extracted from the angular frequency (ω_{rec}) in the Bode phase plots (Figure 9b), using the relation $\tau_e = 1/\omega_{rec}$, gives a lifetime of 93 ms for DSCs based on the PEDOT CEs. This is significantly lower than that of the platinized FTO CEs, 250 ms. This may explain the slightly lower V_{oc} value obtained using PEDOT CEs. As shown by eqs 1−3, the injected electron will be engaged in three different recombination processes with the oxidized redox couple species as well as with the radical species formed from the WE or CE. Therefore, the effective reduction of oxidized species on the CE could increase the concentration of radical species in the electrolytes (see eq 5) accelerating the recombination eq 3. This may explain the unexpected indirect effect of the CE material on recombination losses at the WE.

Recombination processes:

$$R{-}S{-}S{-}R + WE(e^-) \rightarrow R{-}S^- + R{-}S^{\cdot} \quad (1)$$

$$R{-}S{-}S{-}R + WE(2e^-) \rightarrow 2R{-}S^- \quad (2)$$

$$R{-}S^{\cdot} + WE(e^-) \rightarrow R{-}S^- \quad (3)$$

Reduction processes:

$$R{-}S{-}S{-}R + CE(2e^-) \rightarrow 2R{-}S^- \quad (4)$$

$$R{-}S{-}S{-}R + CE(e^-) \rightarrow R{-}S^- + R{-}S^{\cdot} \quad (5)$$

Noticeably, the semicircle originating from the PEDOT CE significantly overlaps with the WE semicircle in PEDOT-based DSCs. Therefore, it is difficult to accurately fit the Nyquist plot data to extract a fully reliable CE resistance. Therefore, EIS investigations of the thin-layer CE//electrolyte A//CE systems were employed under −0.7 V (Figures S4 and S5 of the Supporting Information) and 0 V (Figure 10) bias voltage in order to extract the CE resistance. As shown in Figure 10, the Nyquist plots should consist of the resistance originating from the CE and from the electrolyte, denoted Warburg (frequency-independent) impedance.[3] The latter can be clearly observed at −0.7 V bias voltage and is very low, 5 Ω. It means that the diffusion of the redox couple components in the DSC electrolytes

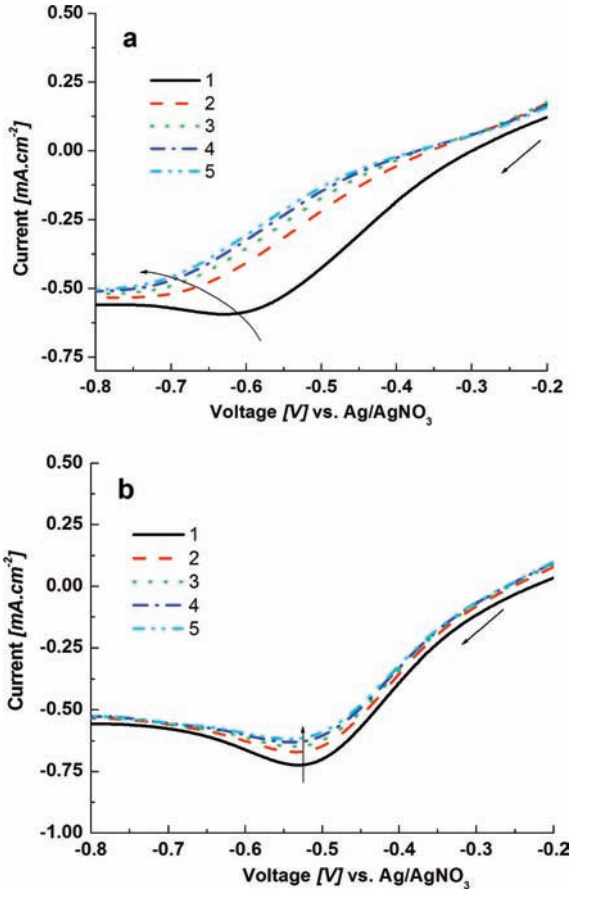

Figure 12. Five cycles of LSV of platinized FTO (a) and PEDOT (b) in 2 mM **1**, 0.1 M $LiClO_4$ in MeCN solution.

studied here is sufficiently high. By fitting the Nyquist plots obtained at 0 V bias voltage to an electrochemical model, it can be deduced that PEDOT as CE materials displays an average charge-transfer resistance on the electrolyte/CE interface (R_{CE}) of 45 Ω. This is considerably lower than that of DSCs with the platinized FTO CE giving an R_{CE} of 355 Ω, which is almost 8 times higher. This implies that the reduction of **1** is

dx.doi.org/10.1021/ja2030933 |J. Am. Chem. Soc. 2011, 133, 9413–9422

Table 2. Photovoltaic Properties of DSCs Containing the Electrolytes IL1 and IL2 under Different Intensity Light Illumination[a]

electrolyte	light intensity[b] [sun]	J_{sc} [mA·cm^{-2}]	V_{oc} [mV]	*ff* [%]	η [%]
IL1	0.1	0.82	652	0.65	3.4
	1	2.76	714	0.37	0.7
IL2	0.1	0.72	640	0.17	0.8
	1	0.96	708	0.19	0.1

[a] The thickness of the TiO_2 film is 6 μm transparent layer. [b] One sun is equal to 100 mW·cm^{-2}.

much less disfavored on the PEDOT surface than on the platinized FTO surface.

To further elucidate the essential differences between the PEDOT and the platinized FTO with respect to reduction of **1**, linear sweep voltammetry (LSV) was performed using a 0.1 M $LiClO_4$ in MeCN solution at a sweep rate of 50 mV·s^{-1} over the potential range from 0 to −0.8 V and with 2 mM **1** employing the PEDOT and platinized FTO as working electrodes. As references, also LSV for bare FTO (Figure 11c) and PEDOT (Figure 11d) in an analogous electrolyte with and without **1** added was included, respectively.

As shown in Figure 11a, the PEDOT electrode renders an obvious reduction peak at −0.52 V, which is ascribed to the reduction peak of **1**. The platinized FTO working electrode shows a reduction peak of **1** at −0.61 V (Figure 11b). Futhermore, the PEDOT electrode shows higher reduction current density of 0.74 mA·cm^{-2} than platinized FTO, 0.58 mA·cm^{-2}. In addition, as shown in Figure 12a, and in contrast to the PEDOT electrode, the potential of **1** reduction using the platinized FTO electrode is not constant upon cycling and shifts to more negative potentials ending at −0.72 V. Such an effect could be explained by the adsorption of the reduced species onto the Pt nanoparticle surfaces, which may inhibit the reduction of **1**. Therefore, in continuously operating DSCs, an adsorption process on the CE could cause significant degradation of performance with time. However, this phenomenon was not observed for the PEDOT electrode for which the reduction peak of **1** was constant at −0.52 V upon voltage cycling (Figure 12b). The less effective reduction ability (low reduction current density) and a more negative reduction potential of **1** on the platinized FTO surface may decrease the reduction rate of **1** and may thus constitute the main reason for the lower *ff* observed in the DSCs.

4. Solvent-Free and Solvated Ionic Liquid Electrolytes. Solvent-free iodide ionic liquid (IL) electrolytes have been employed successfully in DSCs showing the potential of commercial application because of the high efficiency and nonvolatile properties.[50−56] Fortunately, the thiolates $\mathbf{1a}^-$ and $\mathbf{1b}^-$ are pure ILs at room temperature, which provide us with a chance to study the solvent-free thiolate IL electrolytes in DSCs for the first time. The electrolytes IL1 and IL2 were prepared through dissolving 0.2 M **1** in $\mathbf{1a}^-$ and $\mathbf{1b}^-$, respectively.

Table 2 shows the best photovoltaic properties of DSCs based on IL1 and IL2 under different light intensity illumination, 1 and 0.1 sun, respectively. The *J*−*V* curves (0.1 sun) and the IPCE spectra of DSCs based on the two different electrolytes are shown in Figure 13. As we can learn from these data, efficiencies of DSCs based on these IL electrolytes benefit from lower light intensities. This result could probably imply that the mass

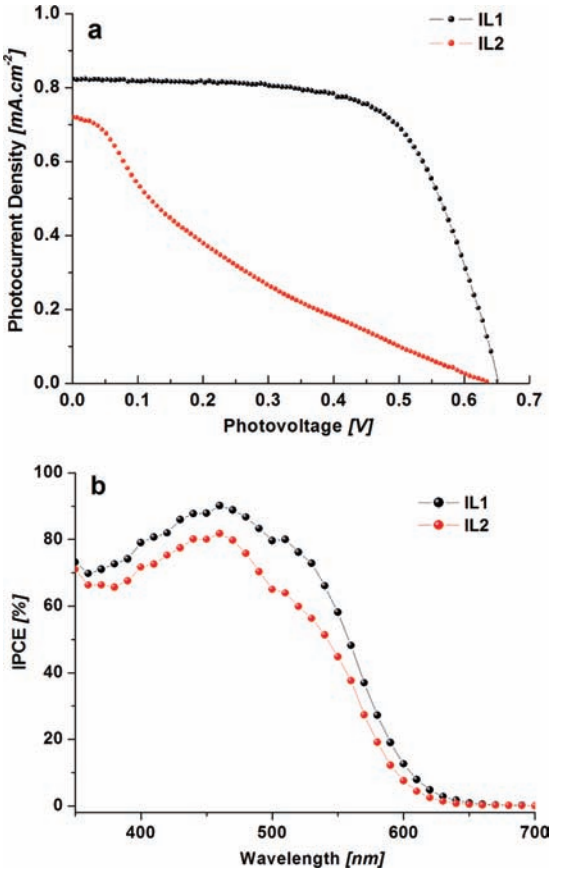

Figure 13. The *J*−*V* curves (0.1 sun) and IPCE spectra of DSCs containing the electrolytes IL1 and IL2.

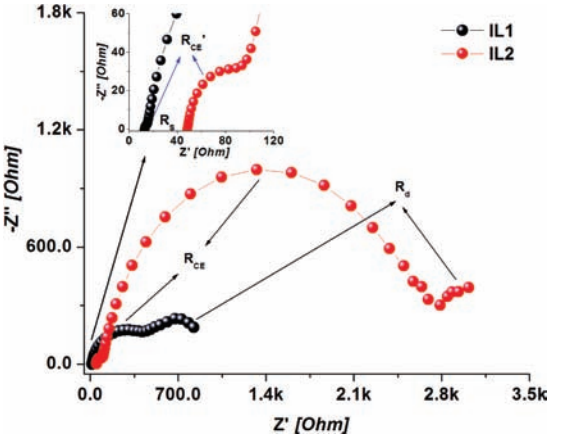

Figure 14. Nyquist plots of PEDOT//IL electrolyte//PEDOT systems with −0.2 V bias voltage.

transport of the redox couple in the electrolytes plays an important role with respect to the efficiencies of the DSC devices. Under 0.1 sun illumination, the DSCs based on IL1 show the best efficiency of 3.4% indicating a potential for indoor applications. As shown in Figure 13, in comparison to the electrolyte IL1, the DSCs based on the electrolyte IL2 show slightly lower photocurrent as well as IPCE values but a similar photovoltage and a lower fill factor resulting in the much lower efficiency observed to 0.8% under 0.1 sun illumination. The disappointing *ff* values are

dx.doi.org/10.1021/ja2030933 |*J. Am. Chem. Soc.* 2011, 133, 9413–9422

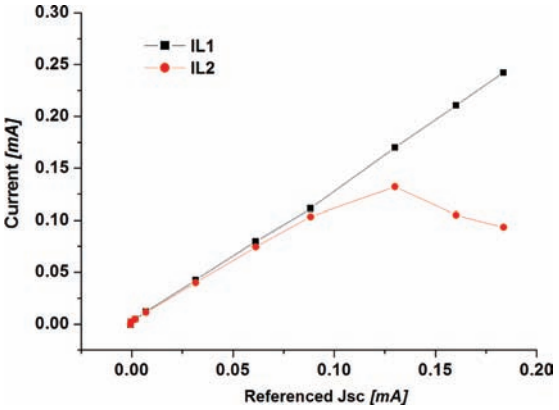

Figure 15. Light-intensity dependence of the current density under short-circuit conditions for DSCs containing the IL electrolytes.

likely to be caused by the counter electrode or diffusion resistances in the electrolyte. To test this hypothesis, EIS of the thin-layer systems (PEDOT//IL electrolyte//PEDOT) based on the electrolytes IL1 and IL2 was performed with a series of bias voltage (Figure S6 of the Supporting Information). At a −0.2 V bias voltage (see Figure 14), the electrolyte reduction characteristics on the CE and the electrolyte diffusion resistance can be clearly observed in the Nyquist plots.

Consequently, the PEDOT//IL electrolyte//PEDOT systems based on the electrolytes IL1 and IL2 were investigated and were compared under the same applied bias voltage −0.2 V. All of the resistances extracted for the system, including the series resistance (R_s) from the conduction through the conducting glass at the WE and CE, the counter electrode resistances consisting of FTO/PEDOT (R_{CE}') and PEDOT/electrolyte (R_{CE}) resistances, and the electrolyte diffusion resistance (R_d) can be clearly observed and separated in frequency space. By fitting the Nyquist plots to a suitable electrochemical model, the corresponding resistance data can be obtained. The R_s and R_{CE}', 48 Ω and 70 Ω, obtained from the model based on the electrolyte IL2 is much higher than the values obtained from the systems based on the electrolyte IL1, 13 Ω and 4 Ω. Especially, the R_{CE} value, 2600 Ω, obtained from the model based on the electrolyte IL2 is much higher than that of the electrolyte IL1, 510 Ω. This means that the **1** component in DSCs containing the electrolyte IL2 is far less easily reduced by the PEDOT CE than cells based on the organic solvent-based electrolyte A (vide supra). However, the concentration of **1** in the electrolytes IL1 and IL2 is the same, and the PEDOT CEs are also the same. Consequently, the difference in R_{CE} between the electrolytes IL1 and IL2 is probably caused by the viscosity of the ionic liquids, which can affect the mass transport of **1** in the electrolytes as well as within the solvated PEDOT film. Viscosity measurements for these two ionic liquids were carried out, and the results show that the viscosity of $\mathbf{1b}^-$ is ca. 1300 cP, which is almost 12 times higher than that of $\mathbf{1a}^-$, ca. 100 cP. Therefore, the larger counter electrode resistance could presumably be caused by the higher viscosity of the ionic-liquid solvents. Also, the light-intensity dependence of the current density under short-circuit conditions for DSCs (Figure 15) based on the IL electrolytes shows that cells containing the electrolyte IL2 give worse restrictions in mass transport than the electrolyte IL1 even under low-light intensity. Turning the attention to the R_d, the model based on the electrolyte IL1 renders a value of 360 Ω. Unfortunately, for the IL2-based model, only a portion of the electrolyte diffusion semicircle can be observed. Thus, it is difficult to fit the semicircle to get accurate data. The estimated R_d of the IL2-based model is ca. 700 Ω, which is also higher than that obtained from the IL1 model. The result is in coherence with the higher viscosity observed for the electrolyte IL2. All the observed higher resistances of IL2-based system result in a lower *ff* as well as in a lower photocurrent.

To decrease the viscosity of the IL electrolytes, we also introduced the concept of solvated ionic liquids to the experiments. When the thiolate $\mathbf{1}^-$ is mixed with 1,2-dimethylimidazole under heating, a solvated ionic liquid (SIL) forms. In addition, another SIL also can be formulated when phenol, as a hydrogen-bond donor, is mixed with $\mathbf{1}^-$. For the traditional iodine-based electrolyte, similar, so-called eutectic solvents (ESs) have been used as a promising strategy to prepare a conductive, less flammable, and less volatile solvent with a low melting point (m.p.) and a high boiling point (b.p.)[50,57] and good DSC performance. Although the viscosity of the SILs is significantly decreased, the best efficiency is only 1.2% obtained for the phenol component-based DSCs with a J_{sc} of 0.7 mA·cm^{-2}, V_{oc} of 498 mV, and *ff* of 0.32 under 0.1 sun illumination. According to the detailed investigation of SIL-based electrolytes (shown in the Supporting Information), we note that the photovoltaic properties of DSCs based on SILs strongly depend on the components used. The positive shift of the TiO_2 CB of phenol offers a better injection efficiency giving a higher overall conversion efficiency in spite of the lower open-circuit voltage caused by such a shift.

■ CONCLUSIONS

In summary, a series of thiolate/disulfide redox couples with weak absorption in the visible light region have been synthesized and applied in organic dye (TH305) sensitized solar cells. The $\mathbf{1}^-/\mathbf{1}$ redox couple with platinized FTO CE provides the best efficiency (η) of 4.6% with a short-current density (J_{sc}) of 12.3 mA·cm^{-2}, an open-circuit voltage (V_{oc}) of 750 mV, and a fill factor (*ff*) of 0.50 under AM 1.5G, 100 mW·cm^{-2} simulated sun light illumination (1 sun). The large charge-transfer resistance at the electrolyte/platinized FTO interface limits the *ff* value of DSCs based on this electrolyte. An alternative CE material, the organic poly(3,4-ethylenedioxythiophene) (PEDOT) film, deposited on a conducting glass substrate by electrochemical polymerization and used as CE in DSCs has been shown to outperform the standard platinized FTO-type of CE for a thiolate/disulfide-type of redox couple. This experiment presents a DSC model based on all-organic dye, redox couple ($\mathbf{1}^-/\mathbf{1}$), and CE, and the most important result is a promising efficiency of 6.0% with a *ff* of 0.65 achieved under standard simulated 1 sun illumination. As compared to a platinized FTO CE, the PEDOT-based film shows considerably lower charge-transfer resistance at the electrolyte/PEDOT interface and also offers a lower potential of reduction of **1**. In combination, this gives a higher *ff* value resulting in a higher conversion efficiency in such DSCs. Furthermore, the concepts of pure and solvated ionic liquids were introduced to this kind of thiolate/disulfide redox-couple-based DSCs for the first time. The best efficiency of 3.4% was achieved by DSCs based on the pure ionic liquid electrolyte with $\mathbf{1a}^-/\mathbf{1}$ redox couple under 10 mW·cm^{-2} (0.1 sun) illumination. Future work will focus on strategies to decrease the electrolyte mass-transport limitations and to improve the chemical stability of this kind of electrolyte by structral modification as well as by optimization of electrolyte composition.

■ ASSOCIATED CONTENT

Supporting Information. Experimental section; electrochemical data for different redox couples; the electrochemical curves and data of different redox couples; UV−vis spectrum and presumed structure of the prepared PEDOT material; Nyquist plots of DSCs containing the electrolyte A based on different PEDOT CEs; the EIS of thin-layer cells Pt CE//electrolyte A//Pt CE and PEDOT CE//electrolyte A//PEDOT CE with −0.7 V bias voltage; the EIS of thin-layer cells PEDOT//IL1//PEDOT and PEDOT//IL1//PEDOT at different applied bias voltages; the collection of photovoltaic properties of DSCs based on different dyes, counter electrodes and electrolytes; the DSC photovoltaic properties of different concentrations of $\mathbf{1}^-$ using PEDOT as counter electrode; $J-V$ curves of N719-based DSCs using different electrolytes and counter electrodes; the photovoltaic curves and properties of DSCs based on thiolate ionic liquid electrolyte IL2 with different thickness TiO_2 films under 10 $mW \cdot cm^{-2}$ sunlight illumination; light-intensity dependence of the current density under short-circuit conditions for DSCs with SIL electrolytes; charge extraction and electron lifetime of DSCs based on the electrolytes IL1 and IL2; detailed investigations of solvated ionic liquid electrolytes. This material is available free of charge via the Internet at http://pubs.acs.org.

■ AUTHOR INFORMATION

Corresponding Author
larsa@kth.se; lichengs@kth.se

■ ACKNOWLEDGMENT

This work was supported by the Swedish Research Council, the Swedish Energy Agency, and the Knut & Alice Wallenberg Foundation. Z. Y. also would like to acknowledge the China Scholarship Council (CSC) for financial support. We would like to thank Kazuteru Nonomura (Uppsala University) for helpful discussions and Dr. Xiao Jiang (KTH) for supplying the TiO_2 paste.

■ REFERENCES

(1) O'Regan, B.; Grätzel, M. *Nature* **1991**, *353*, 737–740.
(2) Hagfeldt, A.; Boschloo, G.; Sun, L.; Kloo, L.; Pettersson, H. *Chem. Rev.* **2010**, *110*, 6595–6663.
(3) Wang, M.; Chamberland, N.; Breau, L.; Moser, J.-E.; Humphry-Baker, R.; Marsan, B.; Zakeeruddin, S. M.; Grätzel, M. *Nat. Chem.* **2010**, *2*, 385–389.
(4) Nusbaumer, H.; Moser, J.-E.; Zakeeruddin, S. M.; Nazeeruddin, M. K.; Grätzel, M. *J. Phys. Chem. B* **2001**, *105*, 10461–10464.
(5) Sapp, S. A.; Elliott, C. M.; Contado, C.; Caramori, S.; Bignozzi, C. A. *J. Am. Chem. Soc.* **2002**, *124*, 11215–11222.
(6) Nusbaumer, H.; Zakeeruddin, S. M.; Moser, J.-E.; Grätzel, M. *Chem.—Eur. J.* **2003**, *9*, 3756–3763.
(7) Cazzanti, S.; Caramori, S.; Argazzi, R.; Elliott, C. M.; Bignozzi, C. A. *J. Am. Chem. Soc.* **2006**, *128*, 9996–9997.
(8) Gibson, E. A.; Smeigh, A. L.; Le Pleux, L.; Fortage, J.; Boschloo, G.; Blart, E.; Pellegrin, Y.; Odobel, F.; Hagfeldt, A.; Hammarström, L. *Angew. Chem., Int. Ed.* **2009**, *48*, 4402–4405.
(9) Caramori, S.; Husson, J.; Beley, M.; Bignozzi, C. A.; Argazzi, R.; Gros, P. C. *Chem.—Eur. J.* **2010**, *16*, 2611–2618.
(10) Feldt, S. M.; Gibson, E. A.; Gabrielsson, E.; Sun, L.; Boschloo, G.; Hagfeldt, A. *J. Am. Chem. Soc.* **2010**, *132*, 16714–16724.
(11) Wang, H.; Nicholson, P. G.; Peter, L.; Zakeeruddin, S. M.; Grätzel, M. *J. Phys. Chem. C* **2010**, *114*, 14300–14306.
(12) Daeneke, T.; Kwon, T.-H.; Holmes, A. B.; Duffy, N. W.; Bach, U.; Spiccia, L. *Nat. Chem* **2011**, *3*, 213–217.
(13) Bai, Y.; Yu, Q.; Cai, N.; Wang, Y.; Zhang, M.; Wang, P. *Chem. Commun.* **2011**, *47*, 4376–4378.
(14) Wang, Z.-S.; Sayama, K.; Sugihara, H. *J. Phys. Chem. B* **2005**, *109*, 22449–22455.
(15) Teng, C.; Yang, X.; Yuan, C.; Li, C.; Chen, R.; Tian, H.; Li, S.; Hagfeldt, A.; Sun, L. *Org. Lett.* **2009**, *11*, 5542–5545.
(16) Rani, S.; Suri, P.; Mehra, R. M. *Prog. Photovolt: Res. Appl.* **2010**, *19*, 180–186.
(17) Teng, C.; Yang, X.; Li, S.; Cheng, M.; Hagfeldt, A.; Wu, L.; Sun, L. *Chem.—Eur. J.* **2010**, *16*, 13127–13138.
(18) Oskam, G.; Bergeron, B. V.; Meyer, G. J.; Searson, P. C. *J. Phys. Chem. B* **2001**, *105*, 6867–6873.
(19) Wang, P.; Zakeeruddin, S. M.; Moser, J.-E.; Humphry-Baker, R.; Grätzel, M. *J. Am. Chem. Soc.* **2004**, *126*, 7164–7165.
(20) Bergeron, B. V.; Marton, A.; Oskam, G.; Meyer, G. J. *J. Phys. Chem. B* **2005**, *109*, 937–943.
(21) Ning, Z.; Tian, H.; Qin, H.; Zhang, Q.; Ågren, H.; Sun, L.; Fu, Y. *J. Phys. Chem. C* **2010**, *114*, 15184–15189.
(22) Li, L.; Yang, X.; Zhao, J.; Gao, J.; Hagfeldt, A.; Sun, L. *J. Mater. Chem.* **2011**, *21*, 5573–5575.
(23) Gregg, B. A.; Pichot, F.; Ferrere, S.; Fields, C. L. *J. Phys. Chem. B* **2001**, *105*, 1422–1429.
(24) Snaith, H. J.; Zakeeruddin, S. M.; Wang, Q.; Pechy, P.; Grätzel, M. *Nano Lett.* **2006**, *6*, 2000–2003.
(25) Li, D.; Li, H.; Luo, Y.; Li, K.; Meng, Q.; Armand, M.; Chen, L. *Adv. Funct. Mater.* **2010**, *20*, 3358–3365.
(26) Tian, H.; Jiang, X.; Yu, Z.; Kloo, L.; Hagfeldt, A.; Sun, L. *Angew. Chem., Int. Ed.* **2010**, *49*, 7328–7331.
(27) Zaban, A.; Micic, O. I.; Gregg, B. A.; Nozik, A. J. *Langmuir* **1998**, *14*, 3153–3156.
(28) Pichot, F.; Gregg, B. A. *J. Phys. Chem. B* **2000**, *104*, 6–10.
(29) Zhang, Z.; Chen, P.; Murakami, T. N.; Zakeeruddin, S. M.; Grätzel, M. *Adv. Funct. Mater.* **2008**, *18*, 341–346.
(30) U.S. Patent 20080041438, 2007.
(31) WO Patent 2007109907, 2008.
(32) Liu, Y.; Jennings, J. R.; Parameswaran, M.; Wang, Q. *Energy Environ. Sci.* **2010**10.1039/c1030ee00519c.
(33) Kiya, Y.; Henderson, J. C.; Hutchison, G. R.; Abruña, H. D. *J. Mater. Chem.* **2007**, *17*, 4366–4376.
(34) Kiya, Y.; Hatozaki, O.; Oyama, N.; Abruña, H. D. *J. Phys. Chem. C* **2007**, *111*, 13129–13136.
(35) Tian, H.; Yang, X.; Cong, J.; Chen, R.; Liu, J.; Hao, Y.; Hagfeldt, A.; Sun, L. *Chem. Commun.* **2009**, 6288–6290.
(36) Hong, W.; Xu, Y.; Lu, G.; Li, C.; Shi, G. *Electrochem. Commun.* **2008**, *10*, 1555–1558.
(37) Ahmad, S.; Yum, J.-H.; Xianxi, Z.; Grätzel, M.; Butt, H.-J.; Nazeeruddin, M. K. *J. Mater. Chem.* **2010**, *20*, 1654–1658.
(38) Pringle, J. M.; Armel, V.; MacFarlane, D. R. *Chem. Commun.* **2010**, *46*, 5367–5369.
(39) Lee, K. S.; Lee, H. K.; Wang, D. H.; Park, N.-G.; Lee, J. Y.; Park, O. O.; Park, J. H. *Chem. Commun.* **2010**, *46*, 4505–4507.
(40) Saito, Y.; Kitamura, T.; Wada, Y.; Yanagida, S. *Chem. Lett.* **2002**, 1060–1061.
(41) Yanagida, S.; Yu, Y.; Manseki, K. *Acc. Chem. Res.* **2009**, *42*, 1827–1838.
(42) Manseki, K.; Jarernboon, W.; Youhai, Y.; Jiang, K.-J.; Suzuki, K.; Masaki, N.; Kim, Y.; Xia, J.; Yanagida, S. *Chem. Commun.* **2011**, *47*, 3120–3122.
(43) Senadeera, R.; Fukuri, N.; Saito, Y.; Kitamura, T.; Wada, Y.; Yanagida, S. *Chem. Commun.* **2005**, 2259–2261.
(44) Xia, J.; Masaki, N.; Lira-Cantu, M.; Kim, Y.; Jiang, K.; Yanagida, S. *J. Am. Chem. Soc.* **2008**, *130*, 1258–1263.
(45) Saito, Y.; Azechi, T.; Kitamura, T.; Hasegawa, Y.; Wada, Y.; Yanagida, S. *Coord. Chem. Rev.* **2004**, *248*, 1469–1478.
(46) Kim, Y.; Sung, Y.-E.; Xia, J.-B.; Lira-Cantu, M.; Masaki, N.; Yanagida, S. *J. Photochem. Photobiol., A: Chem.* **2008**, *193*, 77–80.

(47) Jansen, M.; Rabe, H.; Strehless, A.; Dieler, S.; Debus, F.; Dannhardt, G.; Akabas, M. H.; Lueddens, H. *J. Med. Chem.* **2008**, *51*, 4430–4448.
(48) Hagberg, D. P.; Edvinsson, T.; Marinado, T.; Boschloo, G.; Hagfeldt, A.; Sun, L. *Chem. Commun.* **2006**, 2245–2247.
(49) Fabregat-Santiago, F.; Bisquert, J.; Garcia-Belmonte, G.; Boschloo, G.; Hagfeldt, A. *Sol. Energy Mater. Sol. Cells* **2005**, *87*, 117–131.
(50) Bai, Y.; Cao, Y.; Zhang, J.; Wang, M.; Li, R.; Wang, P.; Zakeeruddin, S. M.; Grätzel, M. *Nat. Mater.* **2008**, *7*, 626–630.
(51) Papageorgiou, N.; Athanassov, Y.; Armand, M.; Bonhote, P.; Pettersson, H.; Azam, A.; Grätzel, M. *J. Electrochem. Soc.* **1996**, *143*, 3099–3108.
(52) Zakeeruddin, S. M.; Grätzel, M. *Adv. Funct. Mater.* **2009**, *19*, 2187–2202.
(53) Yu, Z.; Gorlov, M.; Nissfolk, J.; Boschloo, G.; Kloo, L. *J. Phys. Chem. C* **2010**, *114*, 10612–10620.
(54) Wang, P.; Zakeeruddin, S. M.; Comte, P.; Exnar, I.; Grätzel, M. *J. Am. Chem. Soc.* **2003**, *125*, 1166–1167.
(55) Kubo, W.; Kitamura, T.; Hanabusa, K.; Wada, Y.; Yanagida, S. *Chem. Commun.* **2002**, 374–375.
(56) Kuang, D.; Wang, P.; Ito, S.; Zakeeruddin, S. M.; Grätzel, M. *J. Am. Chem. Soc.* **2006**, *128*, 7732–7733.
(57) Jhong, H.-R.; Wong, D. S.-H.; Wan, C.-C.; Wang, Y.-Y.; Wei, T.-C. *Electrochem. Commun.* **2009**, *11*, 209–211.